

In Vivo Measurement of Swine Endocardial Convective Heat Transfer Coefficient

Chanchana Tangwongsan, James A. Will, John G. Webster*, *Life Fellow, IEEE*, Kenneth L. Meredith, Jr., and David M. Mahvi

Abstract—We measured the endocardial convective heat transfer coefficient h at 22 locations in the cardiac chambers of 15 pigs *in vivo*. A thin-film Pt catheter tip sensor in a Wheatstone-bridge circuit, similar to a hot wire/film anemometer, measured h . Using fluoroscopy, we could precisely locate the steerable catheter sensor tip and sensor orientation in pigs' cardiac chambers. With flows, h varies from 2500 to 9500 W/m²·K. With zero flow, h is approximately 2400 W/m²·K. These values of h can be used for the finite element method modeling of radiofrequency cardiac catheter ablation.

Index Terms—Cardiac radiofrequency ablation, convective heat transfer coefficient, heat convection, endocardial convective heat transfer coefficient, radiofrequency ablation.

I. INTRODUCTION

ACCORDING to the American Heart Association [24], as many as two million people in the United States suffer from atrial fibrillation and more than 100 000 people suffer from tachycardia. radiofrequency (RF) catheter cardiac ablation has been successfully used for the treatment of these cardiac arrhythmias as a preferable alternative of the conventional “Maze” operation (in which long surgical cuts interrupt excitation pathways) and drug therapy because of its controllability, high efficacy, low complication rate, and minimal invasiveness [2], [3], [9], [10]–[15], [19]. In order to improve the electrodes and enhance the success rate of RF catheter ablation, researchers have performed finite element method (FEM) modeling of RF catheter ablation [6], [7], [18]–[20], [22]. The value of endocardial convective heat transfer coefficient (h) is important to accurately simulate heat loss from the endocardium since the blood flow in the cardiac chambers carries away a large amount of heat from the ablation site during the ablation [6], [19], [20]. Researchers have used the value of h ranging from 44 to 6090 W/m²·K for different locations in the cardiac chambers [1], [6], [7], [8], [13], [14], [18], [20]. However, none of these values came from *in vivo*

measurements in animals. Bhavaraju obtained the values of h from *in vitro* experiments [1]. Shahidi *et al.* and Labonte estimated the values of h from mathematical calculations assuming the blood flow is laminar [7], [14]. Tungjitkusolmun *et al.* estimated the values of h using the blood velocities in the cardiac chambers obtained by Doppler ultrasound [20]. Jain *et al.* used the value of h of 1800 W/m²·K for their FEM analysis but did not mention their sources of the value of h [6].

Few attempts to measure h *in vivo* have been reported. Bhavaraju [1] constructed a physical model of the swine heart from silicone rubber and embedded thermistors (BR11, Thermometrics Inc.) into the wall of the model heart. He then pumped a blood substitute, consisting of 40% glycerol and 60% water by weight, at various flow rates through the model heart and measured *in vitro* h , in several locations. His experiments yielded values of h ranging from 44 to 3930 W/m²·K. Since his heart model was stiff, and not as flexible as the real heart, at many locations, especially under the valves, his experimental results of h are extremely low and questionable. Santos *et al.* [12], [13] used a Swan–Ganz catheter with a thermistor embedded near its tip to measure h in eight locations in two pigs *in vivo*. The values of h obtained from his measurements range from 510 to 4800 W/m²·K. However, his experimental results are questionable for several reasons. First, the Swan–Ganz catheter he used is neither stiff nor steerable, making it extremely difficult to accurately locate the measuring sites. Second, he did not use fluoroscopy. Third, the orientation of the measuring surface of his catheter could face the endocardial wall instead of the flowing blood during the measurement, which could significantly alter the results. Fourth, because the thermistor that is embedded on the surface of his catheter is as thick as 0.2 mm, the average temperature he measured was different from the surface temperature, which would result in miscalculation of h .

Because we could not find any reliable values of h in previous research, we measured h using a Wheatstone bridge circuit, similar to a hot wire/film anemometer circuit, connecting it to a steerable catheter sensor, using fluoroscopy and using the system to perform *in vivo* measurements of the endocardial convective heat transfer coefficient h in 22 locations inside the cardiac chambers of 15 pigs.

II. METHOD

Fig. 1 shows the flow chart of *in vivo* measurement of h . The test animals (pigs) were prepared for *in vivo* measurement. The

Manuscript received July 21, 2003; revised January 16, 2004. This work was supported by the National Institute of Health (NIH) under Grant HL56413 and Grant DK58839. Asterisk indicates corresponding author.

C. Tangwongsan is with the Department of Electrical Engineering, Chulalongkorn University, Bangkok 10330, Thailand.

J. A. Will is with the Department of Animal Health and Biomedical Sciences, University of Wisconsin, Madison, WI 53706 USA.

*J. G. Webster is with the Department of Biomedical Engineering, University of Wisconsin, Madison, WI 53706 USA (e-mail: webster@engr.wisc.edu).

K. L. Meredith, Jr., and D. M. Mahvi are with the Department of Surgery, University of Wisconsin, Madison, WI 53792 USA.

Digital Object Identifier 10.1109/TBME.2004.828035

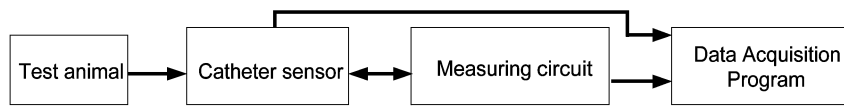


Fig. 1. Flowchart of *in vivo* measurement where the catheter is located inside the pig's cardiac chambers.

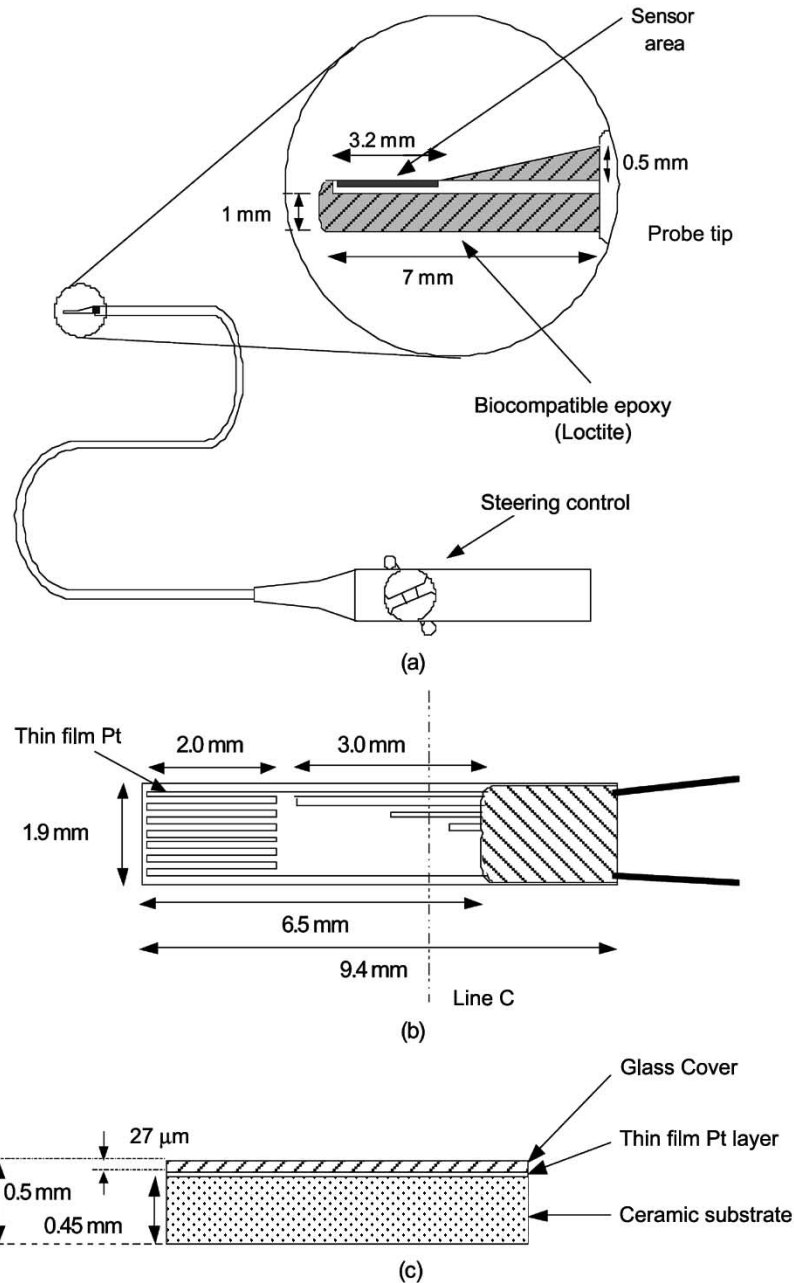


Fig. 2. Catheter sensor. (a) The steerable catheter has Loctite coating except where the thin film Pt sensor (RTD) at its tip is exposed. (b) Top view of the RTD sensor. (c) Cross-sectional view of the RTD sensor through line C.

catheter sensor shown in Fig. 2 was advanced into the cardiac chambers of the pigs to the measuring locations. The catheter sensor was connected to the measuring system, which heated the sensor about $5\text{ }^{\circ}\text{C}$ above the pig's body temperature. The temperature of the heated sensor and the electric power consumed by the sensor were measured and collected by data acquisition programs, Biobench and Labjack. Calculation from those data yielded h [17].

A. Pig Preparation

We obtained pigs, weighing from 12 to 45 kg, from the Department of Animal Science at the University of Wisconsin-Madison (for open chest measurement) and from the University of Wisconsin Hospital, University of Wisconsin-Madison (for measurement under fluoroscopy). The protocol for these studies was approved by the Animal Care and Use Committee and was in compliance with all National Institute of Health (NIH)

guidelines for the humane use of animals in research. The pigs were sedated by injecting Telazol, a narcotic preanesthetic, intramuscularly at an approximate dose of 4 mg/kg. They were then masked to a surgical plane of anesthesia with 5% halothane. The anesthetic was then reduced to 3%–4% and incisions were made with an electrosurgical unit through the skin and underlying tissues to expose the trachea and the sternum. The tracheostomies were achieved by dissection and intubation of the pigs' trachea. The animals were then ventilated and the anesthetic levels adjusted, maintained at oxygen saturation near 100%, and the heart rate was between 80–130 beats/min for the balance of the experiment.

For open chest measurements (without fluoroscopy), the chest of the animal was opened by cutting the sternum from the xiphoid process. Any bleeding from the cuts was ligated or stopped by electrocautery. A surgical retractor kept the chest open, exposing the intact heart within the pericardium. The catheters were introduced into the jugular vein for the right heart measurements and either through the carotid artery or the left atrium directly for the left heart measurements. Placement was verified by palpation and visual observation.

For the measurements under fluoroscopy, the external jugular of the test animal was cannulated and the catheter sensor was advanced to the right atrium and then the right ventricle through the tricuspid valve. The catheter sensor was introduced through the carotid artery to reach the left ventricle and then the left atrium through the mitral valve. Placement of the catheter sensor was verified by fluoroscopy.

B. Catheter Sensor

Fig. 2(a) shows the catheter sensor, which was a modified temperature ablation catheter (Blazer II TM Temp. ablation catheter, Boston Scientific Corporation) with a Pt thin-film resistive temperature sensor (TFD, Omega Engineering, Inc.) as shown in Fig. 2(b) on its tip. The temperature sensor was covered by a thin layer of glass ($\approx 27 \mu\text{m}$) on top of the thin-film Pt to protect it from erosion and any mechanical impact. Another layer of ceramic substrate ($\approx 0.45 \text{ mm}$) was underneath the Pt thin film. The temperature sensor was mounted on the tip of an ablation catheter, and Loctite, a biocompatible epoxy, sealed the electric connection, covering the backside of the sensor and rounding the sharp edges of the sensor. Dr. D. Panescu of the Boston Scientific Corporation supplied the catheter.

C. Measuring System

We used the circuit shown in Fig. 3 [17] to measure h . The measuring circuit, similar to a constant temperature hot wire/film anemometer, is a Wheatstone bridge circuit with the catheter sensor in one of its arms and three wire-wound resistors (1 W) and a precision potentiometer in the other arms. The bridge circuit maintains the resistance of the sensor constant; thus, the temperature of the heated sensor remains constant (in the constant temperature mode) during measurement. The potentiometer is adjusted so the sensor heats 5°C above the flowing fluid temperature.

To acquire the value of h , we measured the voltage across the sensor (V_1) and the voltage across R_1 and R_s (V_A) and recorded

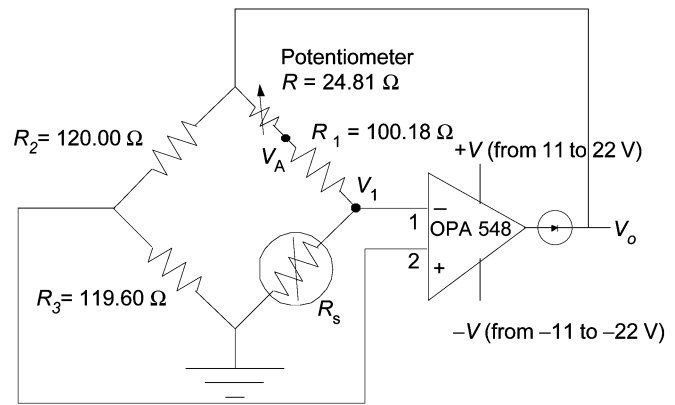


Fig. 3. Circuit diagram of constant temperature measuring system, R_1 , R_2 , and R_3 are wire-wound resistors with 1% tolerance, $\pm 20 \text{ ppm}/^\circ\text{C}$ temperature coefficient. R_s is a resistive temperature detector.

them using the BioBench program and Labjack program. V_A and V_1 were used to determine the current that flows through the sensor. V_1 was also used to determine the resistance and the temperature of the sensor. Once we knew the current, the resistance, and the temperature of the sensor, we could estimate the electric power consumed by the heated sensor. Hence, we calculated h using

$$Q_h = hA(T_s - T_b) \quad (1)$$

where

- Q_h electric power consumed by heating the sensor (W);
- h convective heat transfer coefficient ($\text{W}/\text{m}^2 \cdot \text{K}$);
- A sensor area (m^2);
- T_s temperature of the heated sensor (K);
- T_b temperature of the blood that flows adjacent to the site (K)

However, a correction is needed to obtain a more accurate value of h since there is a glass layer cover on top of the Pt thin film and another layer of ceramic substrate underneath the Pt thin film [17]. Fig. 4(a) shows the equivalent structure of the catheter sensor in the one-dimensional heat transfer through the catheter sensor. Fig. 4(b) shows the electrical analogy. We treat the heat transfer rate (q) as a flow and we calculated the thermal resistances from the thermal conductivity, convective heat transfer coefficient, and thickness of the material and the area of the material. The temperature difference is analogous to the potential difference. The Fourier equation may be written as

$$\text{Heat flow} = \frac{\text{thermal potential difference}}{\text{thermal resistance}} \text{ or } q = \frac{\Delta T_{\text{overall}}}{\Sigma R_{\text{th}}} \quad (2)$$

From Fig. 4(b) and (2), the value of h can be calculated using (3), shown at the bottom of the next page [17], where

- A exposed surface area of the catheter sensor [as shown in Fig. 2(a)] = $3.2 \text{ mm} \times 1.9 \text{ mm} = 6.08 \times 10^{-6} \text{ m}^2$;
- ΔT temperature difference between the heated sensor and the blood (K);
- q electric power consumed by the heated sensor (W);
- R_G thermal resistance of the glass layer = $(d_G)/(k_G A)$ (K/W);

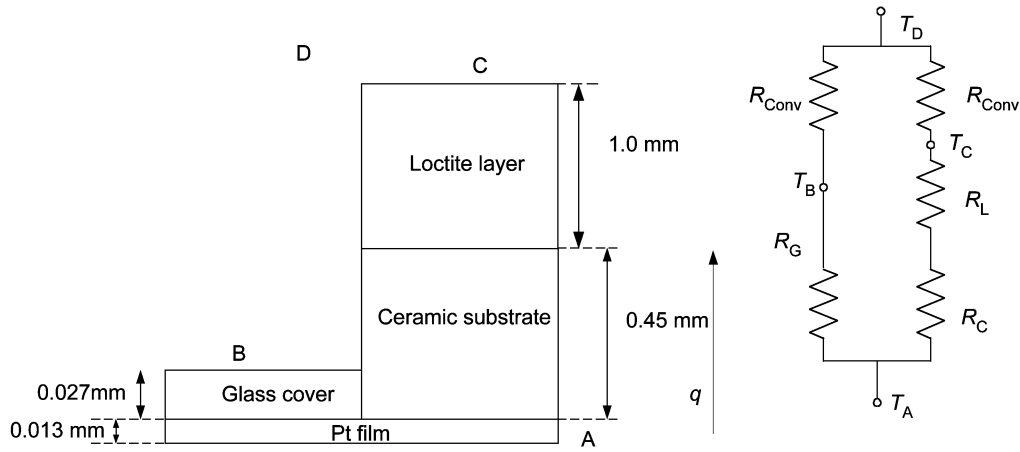


Fig. 4. One-dimensional heat transfer through the catheter sensor. (a) The equivalent structure of the catheter sensor. (b) The electrical analogy.

- R_C thermal resistance of the ceramic substrate = $(d_C)/(k_C A)$ (K/W);
- R_L thermal resistance of the Loctite layer = $(d_L)/(k_L A)$ (K/W);
- d_G thickness of the glass layer = 0.027 mm;
- k_G thermal conductivity of the glass = 1.38 W/m·K;
- d_C thickness of the ceramic substrate = 0.45 mm;
- k_C thermal conductivity of the ceramic = 6.06 W/m·K;
- d_L thickness of the Loctite = 1.00 mm;
- k_L thermal conductivity of the Loctite = 0.55 W/m·K.

D. In Vivo Measurement

In order to perform *in vivo* measurements, the pericardium was opened and the catheters were advanced to the designated measuring sites in the atria, the ventricles, and the valves.

We measured the values of h in 22 locations in the pig's cardiac chambers. The measuring locations in the right atrium were the lateral and the medial walls, the floating position in the right atrium, and at the AV node. For the right ventricle, we measured the floating position in the right ventricle, the lateral and the septal walls, the apex of the right ventricle, the AV node (ventricular side), underneath the tricuspid valve, and the floating position in the tricuspid valve and in the pulmonary valve.

For the left atrium, the measuring locations were the lateral and medial walls of the left atrium and the floating position inside the left atrium. The measuring locations in the left ventricle included the floating position in the left ventricle, the lateral and septal walls, the apex, underneath the mitral valve, and the floating positions in the mitral valve and in the aortic valve.

When we measured the values of h at the endocardial walls under fluoroscopy, we pressed the back of the catheter sensor against the walls leaving the sensing area facing the flowing

blood. We utilized fluoroscopy to ensure the proper orientation of the sensor and the precise measuring sites. Fig. 5 shows the images from fluoroscopy, illustrating the placement of the catheter sensor and the proper orientation of the sensor thin film, which faced the flowing blood in the cardiac chambers. We also ensured that the catheter sensor was not placed in the blood for more than 20 min. After 20 min, the deposition of blood components on the sensor began to affect our measurements (data not shown). We also cleaned the surface of the sensor with water and dried it every time we reinserted the sensor to remove any blood deposition. Each measurement was recorded for at least 30 s using either Biobench or Labjack data acquisition programs. The results were then analyzed using (3) to yield the value of h . Although the placements of the catheter sensor in many locations are next to the wall in the cardiac chambers, not in the floating position, the values of h obtained using (3) are less than 10% different from the more accurate equation (not shown here). Therefore, we only use (3) to yield the value of h in all locations.

III. RESULTS

A. Theoretical Calculation of h in Zero Flow in the Cardiac Chambers

For free convection in still blood (at the body temperature of 39 °C) for vertical planes at an isothermal surface [17], the sensor was heated to a constant 5 °C above the blood temperature. By using the thermal properties of blood [18], [19], [22] and the volume coefficient of expansion β of water, the Grashof number and the Prandtl number are

$$\text{Gr}_f \text{Pr}_f = 260$$

From [4, Fig. 7-7], $\text{Nu}_f = 3.31$ and $\bar{h} = 1200 \text{ W/m}^2 \cdot \text{K}$, where \bar{h} is the average value of h over the exposed area of the sensor.

$$h = \frac{1}{A \left[\left[\frac{\Delta T}{q} - \frac{R_G + R_L + R_C}{2} \right] + \sqrt{\frac{(R_G + R_L + R_C)^2}{4} + \left(\frac{\Delta T}{q} \right)^2 - R_G(R_L + R_C)} \right]} \quad (3)$$

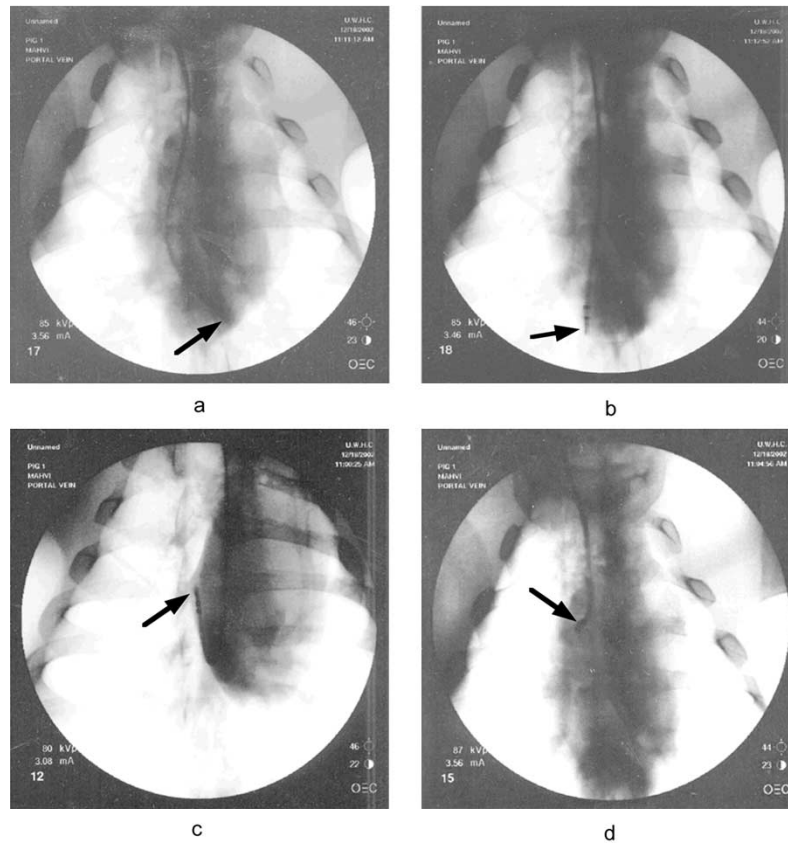


Fig. 5. Fluoroscopy images from the *in vivo* measurements of h : (a) at the apex of right ventricle, (b) at the lateral wall of right ventricle, (c) underneath the tricuspid valve, and (d) at the lateral wall of the right atrium.

TABLE I
EXPERIMENTAL RESULTS OF THE *IN VIVO* ENDOCARDIAL CONVECTIVE HEAT
TRANSFER COEFFICIENT h ($W/m^2 \cdot K$) IN 22 LOCATIONS FROM 15 PIGS

Location	# of data	Median h	Average h	SD
Right atrium (lateral wall)	8	4000	4360	820
Right atrium (medial wall)	1	7900	7900	N/A
Right atrium (floating)	5	7200	7340	1800
Right ventricle (lateral wall)	7	4300	4800	1820
Right ventricle (septum)	6	4750	4780	1200
Right ventricle (apex)	4	5350	5700	1030
Right ventricle (floating)	5	7000	6820	1480
AV node (atrial side)	3	2500	4330	3180
AV node (ventricular side)	5	3900	5660	2790
Tricuspid valve (floating)	3	7500	8000	1320
Tricuspid valve (underneath)	6	6550	6400	2280
Pulmonary valve (floating)	3	8000	7830	1160
Left atrium (lateral wall)	8	5350	5540	1600
Left atrium (medial wall)	1	7000	7000	N/A
Left atrium (floating)	4	9500	9380	710
Left ventricle (lateral wall)	4	4350	4480	1520
Left ventricle (septum)	4	4100	4430	1690
Left ventricle (apex)	4	5700	5900	2000
Left ventricle (floating)	4	8450	8380	2320
Mitral valve (floating)	3	6700	6530	860
Mitral valve (underneath)	4	6800	6830	512
Aortic valve (floating)	2	5500	5500	2260

B. *In Vivo* Experimental Results

Table I shows the experimental results of the *in vivo* measurements in 22 locations in the cardiac chambers of 15 pigs. We pooled the data obtained from both the open chest animals and under fluoroscopy since there were no significant differences

in data. The values of h range from 2500 to 9500 $W/m^2 \cdot K$. We performed at least three measurements at each location (except at the medial walls of the atria and the floating position in the aortic valve) and calculated the median values of h , the average values of h , and the standard deviations of the results from all measurements at each location. Fig. 6 presents the median values of h mapped on a heart diagram. The largest value of h was obtained from the floating position in the left atrium and the smallest value of h was obtained from the right atrial wall near the AV node (AV node in the right atrium). Table II shows the values of h at zero flow in each cardiac chamber measured after the heart stopped. The value of h in each cardiac chamber at zero flow was approximately 2400 ± 50 $W/m^2 \cdot K$. There was no significant difference of the free h measured from each cardiac chamber. Fig. 7 shows the waveforms from the *in vivo* measurements of h at eight locations in the cardiac chambers recorded by the Biobench program.

IV. DISCUSSION

The goal of this project was to obtain accurate *in vivo* measurements of h . Several factors were critical to the design of the probe we utilized. We selected a thin sensor so that the surface temperature was close to the average temperature. We determined the thermal resistance of any backing and protective coating. We needed to ensure that little or no blood components were deposited on the surface of the sensor to avoid added thermal resistance. We considered two alternatives, coating the

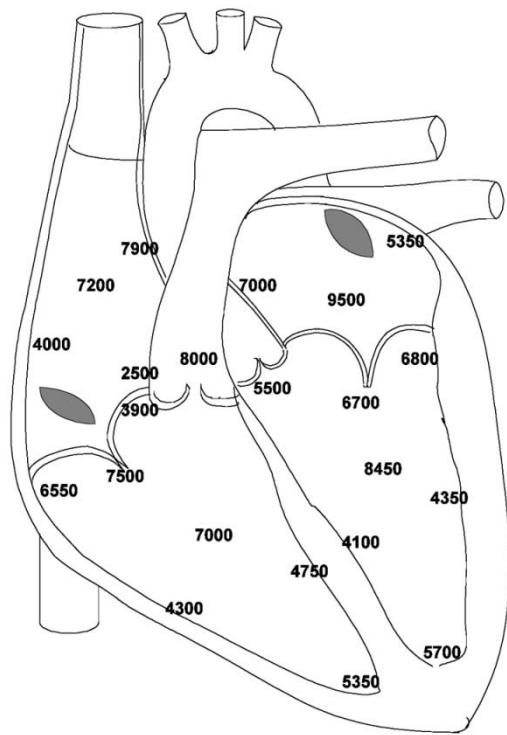


Fig. 6. Median values of h from *in vivo* measurements in 15 pigs in 22 locations mapped on a heart diagram.

TABLE II
EXPERIMENTAL RESULTS OF THE *In Vivo* ENDOCARDIAL CONVECTIVE HEAT TRANSFER COEFFICIENT h ($W/m^2 \cdot K$) AT ZERO FLOW IN EACH CARDIAC CHAMBER

Location	# of data	Median h	Average h	SD
Right atrium	3	2400	2430	58
Right ventricle	4	2300	2380	545
Left atrium	4	2450	2430	96
Left ventricle	4	2300	2280	377

sensor with heparin-carbon solution [21] or frequently cleaning the sensor. Coating with heparin solution is desirable but not very practical since it adds an unknown thermal resistance. As a result, every 20 min we cleaned the sensor to remove any blood deposition during the measurement. Finally, we needed to confirm the location and proper orientation of the sensor. This was accomplished both by palpation in the open chest and by fluoroscopy in the closed chest.

The median values of h are reported in 22 locations in the heart. For the floating position in each chamber, the values of h in the left side of the heart are higher than those in the right side. This is reasonable since blood velocity is higher in the left cardiac chambers [5]. The values of h measured at the endocardial wall in the ventricles and the values of h at the apices of both ventricles are higher than those at the septum and the outer walls. This may reflect that the majority of the blood from both atria flows directly to the apices while a smaller amount of blood with lower velocity flows past the septum and outer walls.

For floating positions in each valve, the highest value of h is at the pulmonary valve ($8000 W/m^2 \cdot K$) and the lowest value of h is at the aortic valve ($5000 W/m^2 \cdot K$). However, theory suggests that higher velocity should yield a higher value of h and the

TABLE III
VELOCITIES OF THE BLOOD IN THE HUMAN HEART AND SOME LARGE VESSELS (CM/S) [5], [22]

Location	Range	Average	Standard deviation
Superior vena cava	28 – 80	51	13
Tricuspid valve	33 – 81	53	12
Pulmonary artery	52 – 131	81	17
Mitral valve	44 – 128	77	16
Ascending aorta	76 – 155	104	19
Descending aorta	70 – 160	101	17

average velocity at the ascending aorta is higher than that at the pulmonary artery [5], [23], as shown in Table III. This low experimental value of h at the aortic valve might result from the improper placement of the catheter sensor in the ascending aorta during the measurement. The catheter sensor might have been close to the wall of the ascending aorta, which has lower blood velocity, instead of floating in the middle of the valve.

Because the beating heart moves and twists with each beat, it is not possible to measure the boundary layer effects as a function of position within the heart chambers. Furthermore, the flow phenomena of blood inside the cardiac chambers are totally different from what would be expected in a solid tube or geometrical-formed container. During ventricular filling in the left ventricle, as soon as the valve opens, the blood from the left atrium flows into the left ventricle and forms vortices [16].

For a zero flow rate, all of the values of h in each cardiac chamber are very similar at approximately $2400 \pm 50 W/m^2 \cdot K$. Although this value is about twice as large as the theoretical calculation value of free convection in the blood mentioned earlier, the lack of variability between measurements suggests that our result is accurate. We measured the values of h when the heart had already stopped its activity; thus, we did not expect any residual flow. However, since the valves inside the cardiac chamber were not fully closed, the blood could still move through the valves due to gravitational force and the remaining pressure inside the cardiac chambers. This slight flow could be the main cause of the high value of h we obtained. Furthermore, some minor inaccuracy of the theoretical calculation might have occurred because the thermal properties we used for the theoretical calculation were the values at $37^\circ C$, since we could not find those values at $39^\circ C$ (pig's body temperature). Finally, we estimated some of the values, such as the volume coefficient of expansion from the value for water since we could find no values measured in blood.

Because of the small size of the sensor, the Grashof or Rayleigh Number and the Reynolds number (for the forced convection flows) are small. Most of the correlations are more reliable at the upper end of the Grashof or Reynolds number ranges, hence better agreement of the experimental data and the theoretical calculation at higher flows.

At the lower flow rate in stagnant liquid (at a low Grashof Number), the experimental flow regime is uncertain. The natural convection correlation assumes a flat vertical surface, no edge effects, constant fluid properties, and no forced convection (fluid movement) at all which are difficult to replicate. Most other experiments in natural convection attempt for relatively large Grashof numbers, therefore the flow is strongly driven by

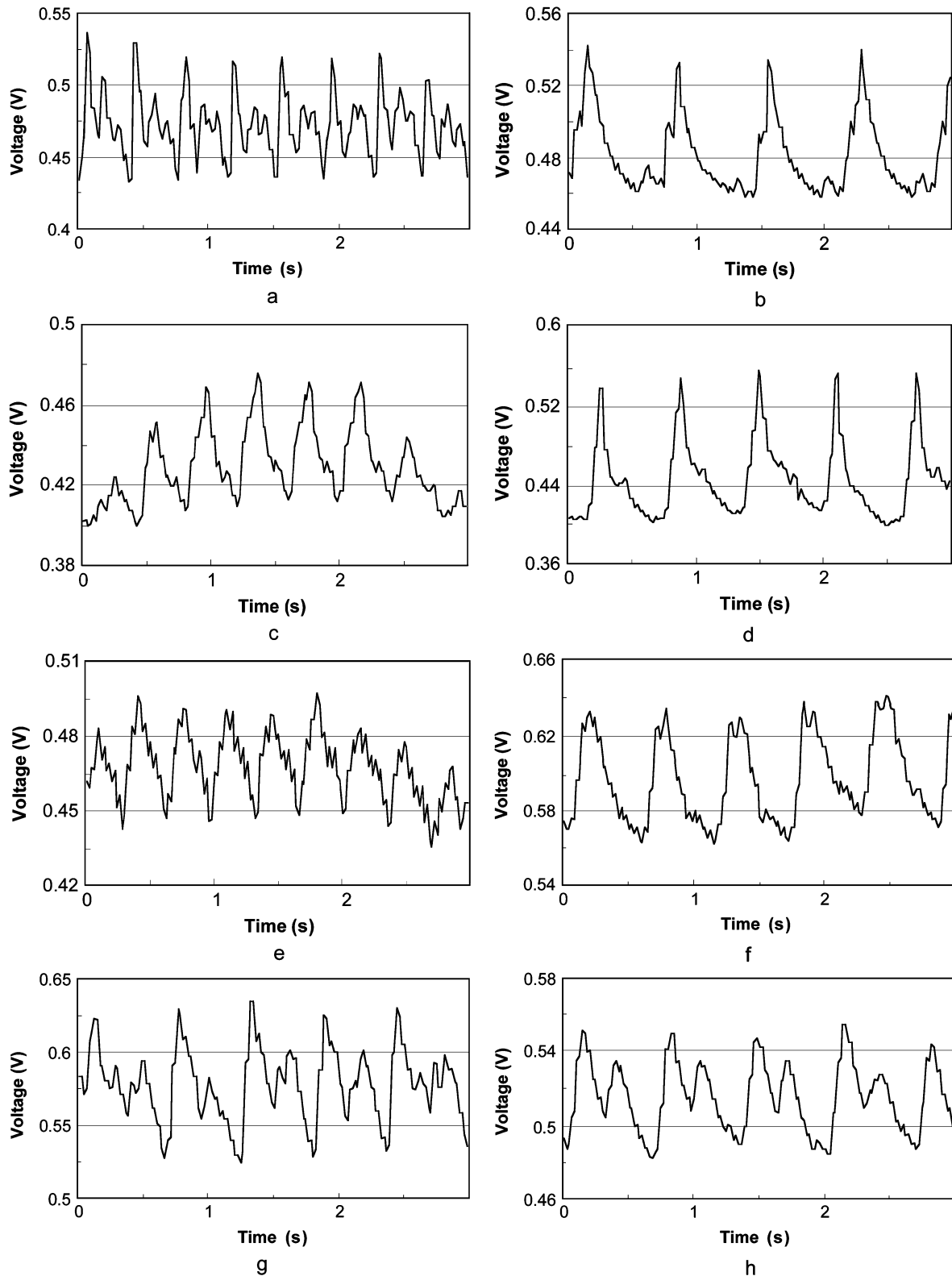


Fig. 7. Waveforms of the voltage across the catheter sensor R_s detected during the *in vivo* measurement of h using the Biobench data acquisition program: (a) in the right atrium, (b) in the left atrium, (c) in the right ventricle, (d) in the left ventricle, (e) in the tricuspid valve, (f) in the mitral valve, (g) in the pulmonary valve, and (h) in the aortic valve. All of the waveforms are not from the same pig; hence there are different heart rates.

free convection with negligible small amounts of forced convection. However, in our case, Gr is small, so normally negligible small forced convection has a big effect and cannot be neglected.

Fig. 7 shows that the waveforms from the *in vivo* measurements of h are very similar to the waveforms from pressure measurements. Fig. 7(h), measured in the aortic valve, shows a sim-

ilar waveform as the aortic pressure recorded by Nerem *et al.* [11].

V. CONCLUSION

This study shows that h can be measured *in vivo* using a hot wire/film anemometer system.

We measured h at 22 locations in the cardiac chambers of 15 pigs. At each location, we measured at least three separate measurements (from different pigs) and calculated the median, average, and the standard deviation. For each measurement, we measured at least 30 s and calculated to yield the average value of h . We also obtained waveforms from each measurement and we found that they are very similar to the waveforms from pressure measurement.

ACKNOWLEDGMENT

The authors would like to thank P. V. Farrell of the Mechanical Engineering Department, University of Wisconsin-Madison, for his helpful suggestions about the theoretical calculation of free convection.

REFERENCES

- [1] N. C. Bhavaraju, "Heat transfer modeling during radiofrequency cardiac ablation in swine myocardium," Ph.D. dissertation, Dept. Biomedical Eng., Univ. Texas, Austin, 2000.
- [2] S. A. Chen, C. E. Chiang, C. T. Tai, S. H. Lee, and M. S. Chang, "Future ablation concepts of tachyarrhythmias," *J. Cardiovasc. Electrophysiol.*, pt. I, vol. 6, no. 10, pp. 852–862, 1995.
- [3] M. Haissaguerre, P. Jais, D. C. Shah, L. Gencel, V. Pradeau, S. Garrigues, S. Chouairi, M. Hocini, P. Le Metayer, R. Roudaut, and J. Clementy, "Right and left atrial radiofrequency catheter therapy of paroxysmal atrial fibrillation," *J. Cardiovasc. Electrophysiol.*, vol. 7, pp. 1132–1144, 1996.
- [4] J. P. Holman, *Heat Transfer*, 8th ed. New York: McGraw-Hill, 1997.
- [5] A. B. Houston and I. A. Simpson, *Cardiac Doppler Ultrasound: A Clinical Perspective*. London, U.K.: Wright, 1988.
- [6] M. K. Jain and P. D. Wolf, "Finite element analysis predicts dose-response relationship for constant power and temperature controlled radiofrequency ablation," in *Proc. 19th Int. Conf.—IEEE/EMBS*, vol. 1, 1997, pp. 165–168.
- [7] S. Labonte, "A computer simulation of radiofrequency ablation of the endocardium," *IEEE Trans. Biomed. Eng.*, vol. 41, pp. 883–890, Sept. 1994.
- [8] —, "Numerical model for radio-frequency ablation of the endocardium and its experimental validation," *IEEE Trans. Biomed. Eng.*, vol. 41, pp. 108–115, 1994.
- [9] C. P. Lau, Y. T. Tai, and P. W. H. Lee, "The effects of radiofrequency ablation versus medical therapy on the quality-of-life and exercise capacity in patients with accessory pathway-medical supraventricular tachycardia: A treatment comparison study," *PACE*, vol. 18, pp. 424–432, 1995.
- [10] M. S. Mirotnik, D. T. Demazumder, J. R. Jones, and D. S. Schwartzman, "Heating distribution of multipolar radiofrequency ablation catheters," in *Proc. 19th Int. Conf.—IEEE/EMBS*, vol. 1, 1997, pp. 157–160.
- [11] R. M. Nerem, W. A. Seed, and N. B. Wood, "An experimental study of the velocity distribution and transition to turbulence in the aorta," *J. Fluid Mech.*, pt. 1, vol. 52, pp. 137–160, 1972.
- [12] I. D. Santos, J. Shah, A. F. da Rocha, J. G. Webster, and J. W. Valvano, "An instrument to measure the heat convection coefficient on the endocardial surface," *Physiol. Meas.*, vol. 24, pp. 321–335, 2003.
- [13] I. D. Santos, J. A. Will, A. F. da Rocha, F. A. de O. Nascimento, J. G. Webster, and J. W. Valvano, "In vivo measurements of heat transfer on the endocardial surface," *Physiol. Meas.*, vol. 24, pp. 793–804, 2003.
- [14] V. Shahidi and P. Savard, "A finite element model for radiofrequency ablation of the myocardium," *IEEE Trans. Biomed. Eng.*, vol. 41, pp. 963–968, Oct. 1994.
- [15] T. P. Stuart, I. A. Nicholson, G. R. Nunn, A. Rees, L. Trieu, M. P. J. Daly, E. M. Wallace, and D. L. Ross, "Effect of atrial radiofrequency ablation designed to cure atrial fibrillation on atrial mechanical function," *J. Cardiovasc. Electrophysiol.*, vol. 11, pp. 77–82, 2000.
- [16] N. Talukder and H. Reul, "Fluid mechanics of natural cardiac valves," in *The Arterial System—Dynamics Control Theory and Regulation*, R. D. Bauer and R. Busse, Eds. Berlin, Germany: Springer-Verlag, 1978, pp. 269–274.
- [17] C. Tangwongsan, "Measurement of *in vitro* endocardial and hepatic convective heat transfer coefficient," Ph.D. dissertation, Dept. Biomed. Eng., Univ. Wisconsin, Madison, 2003.
- [18] S. Tungjitkusolmun, E. J. Woo, H. Cao, J. Z. Tsai, V. R. Vorperian, and J. G. Webster, "Finite element analyses of uniform current density electrodes for radio-frequency cardiac ablation," *IEEE Trans. Biomed. Eng.*, vol. 47, pp. 32–40, Jan. 2000.
- [19] —, "Thermal-electric finite element modeling for radio frequency cardiac ablation: Effects of changes in myocardial properties," *Med. Biol. Eng. Comput.*, vol. 38, pp. 562–568, 2000.
- [20] S. Tungjitkusolmun, V. R. Vorperian, N. Bhavaraju, H. Cao, J. Z. Tsai, and J. G. Webster, "Guidelines for predicting lesion size at common endocardial locations during radio-frequency ablation," *IEEE Trans. Biomed. Eng.*, vol. 48, pp. 194–201, Feb. 2001.
- [21] J. D. Whiffen, R. Dutton, W. P. Young, and V. L. Gott, "Heparin application to graphite-coated intravascular prostheses," *Surgery*, vol. 56, pp. 404–412, 1964.
- [22] E. J. Woo, S. Tungjitkusolmun, H. Cao, J. Z. Tsai, J. G. Webster, V. R. Vorperian, and J. A. Will, "A new catheter design using needle electrode for subendocardial RF ablation of ventricular muscles: Finite element analysis and *in vitro* experiments," *IEEE Trans. Biomed. Eng.*, vol. 47, pp. 23–31, Jan. 2000.
- [23] T. Yamaguchi, S. Kikkawa, T. Yoshikawa, K. Tanishita, and M. Sugawara, "Measurement of turbulence intensity in the center of the canine ascending aorta with a hot-film anemometer," *J. Biomed. Eng.*, vol. 105, pp. 177–187, 1983.
- [24] Heart Disease and Stroke Statistics-2003 Update (2003). [Online]. Available: <http://www.americanheart.org/downloadable/heart/10461207852142003HDSStatsBook.pdf>



Chanchana Tangwongsan was born in Bangkok, Thailand, on January 18, 1974. She received the B.E. degree in electrical engineering from Chulalongkorn University, Bangkok, Thailand, in 1996, and the M.S. and Ph.D. degrees in biomedical engineering from the University of Wisconsin-Madison in 1999 and 2003, respectively.

She is now on the faculty of the Department of Electrical Engineering, Chulalongkorn University. Her research interests include biomedical instrumentation, biosensors, RF cardiac ablation, and hepatic

ablation.



James A. Will received the B.S. degree in agriculture, the M.S. degree in animal science, and the Ph.D. degree in veterinary science from the University of Wisconsin-Madison in 1952, 1953, and 1967, respectively, and the D.V.M. from Kansas State University, Manhattan, in 1960.

Since 1967, he has been with the University of Wisconsin-Madison in the College of Agricultural and Life Sciences, the School of Veterinary Medicine, and the Department of Anesthesiology of the Medical School, serving as Professor and Chairman of Veterinary Science from 1974 to 1978. He became a Professor Emeritus in 2000. He has authored 108 reviewed publications specializing in the pulmonary circulation and cardiopulmonary physiology, pharmacology, and morphology.

Dr. Will is a member of the American Physiological Society and the American Veterinary Medical Association and a Fellow of the Royal Society of Medicine.



John G. Webster (M'59–SM'69–F'86–LF'97) received the B.E.E. degree from Cornell University, Ithaca, NY, in 1953, and the M.S.E.E. and Ph.D. degrees from the University of Rochester, Rochester, NY, in 1965 and 1967, respectively.

He is Professor Emeritus of Biomedical Engineering at the University of Wisconsin-Madison. In the field of medical instrumentation he teaches undergraduate and graduate courses and does research on RF cardiac and hepatic ablation. He is the editor of *Medical Instrumentation: Application and*

Design, 3rd ed. (New York: Wiley, 1998, 3rd ed.), *Encyclopedia of Electrical and Electronics Engineering* (New York: Wiley, 1999), *Bioinstrumentation* (New York: Wiley, 2004), and 20 other books.

Dr. Webster is the recipient of the 2001 IEEE-EMBS Career Achievement Award.



Kenneth L. Meredith, Jr., received the B.S. degree in chemistry and biology from Western Kentucky University, Bowling Green, and the M.D. degree from the University of Louisville, Louisville, KY, in 2000.

He then completed his internship in general surgery at the University of Kentucky (2000–2001). He entered the University of Wisconsin, Madison, as a resident in general surgery (2001–2002). In 2002–2003, he completed a fellowship in surgical oncology. Currently, he is completing general

surgery training at the University of Wisconsin and plans to pursue a career in surgical oncology.



David M. Mahvi received the M.D. degree from the Medical University of South Carolina, Charleston, in 1981.

He then completed the following postgraduate medical clinical training programs at Duke University, Durham, NC: residency in surgery from 1981 to 1983; fellowship in immunology from 1983 to 1985; residency in surgery from 1985 to 1989. In 1989, he joined the Section of Surgical Oncology, Department of Surgery, University of Wisconsin-Madison, where he is now a Professor of Surgery and chief of the

section.

Prof. Mahvi is a member of the University of Wisconsin Comprehensive Cancer Center.